

Observations of z-Dependent Microbunching Harmonic Intensities Using COTR in a SASE FEL*

A. H. Lumpkin, S. G. Biedron⁺, R. J. Dejus, W. J. Berg, M. Borland, Y. C. Chae, M. Erdmann, Z. Huang, K.-J. Kim, Y. Li, J. W. Lewellen, S. V. Milton, E. Moog, V. Sajaev, and B. X. Yang

Advanced Photon Source, Argonne National Laboratory, Argonne, Illinois 60439
USA

Abstract

The nonlinear generation of harmonics in a self-amplified spontaneous emission (SASE) free-electron laser (FEL) continues to be of interest. Complementary to such studies is the search for information on the electron beam microbunching harmonic components, which are revealed by coherent optical transition radiation (COTR) experiments. An initial z-dependent set of data has been obtained with the fundamental at 530 nm and the second harmonic at 265 nm. The latter data were collected after every other undulator in a nine-undulator string. These results are compared to estimates based on GINGER and an analytical model for nonlinear harmonic generation.

The submitted manuscript has been created by the University of Chicago as Operator of Argonne National Laboratory ("Argonne") under Contract No. W-31-109-ENG-38 with the U.S. Department of Energy. The U.S. Government retains for itself, and others acting on its behalf, a paid-up, nonexclusive, irrevocable worldwide license in said article to reproduce, prepare derivative works, distribute copies to the public, and perform publicly and display publicly, by or on behalf of the Government.

⁺ Work partially supported by Max-Laboratory, University of Lund, SE-221 00 Sweden.

*Work supported by U.S. Department of Energy, Office of Basic Energy Sciences under Contract No. W-31-109-ENG-38.

Introduction

The interest in nonlinear generation of harmonics [1-4] in a self-amplified spontaneous emission (SASE) free-electron laser (FEL) continues to grow as experimental results are reported [5,6]. The harmonic aspects are important not only as a test of our understanding of the process, but also because their existence offers a way to generate FEL radiation at shorter wavelengths without increasing the electron beam acceleration capability. The observed growth of the SASE fundamental and second harmonic has been described previously [6]. In this paper we focus on the complementary information on the microbunching harmonic components as revealed through coherent optical transition radiation (COTR) techniques. The description of the longitudinal density modulation that occurs in microbunching is based on the Fourier components at the various harmonics [7,8]. The intensities of radiation seen at the harmonic wavelengths are directly related to such amplitudes. Although we are dealing with a planar undulator system whose SASE radiation couples more strongly to the odd harmonics [4], we have observed a clean signature (~1% of the fundamental) of the second harmonic intensities of the COTR at 265 nm. We have also performed these experiments with z-dependent sampling after every other undulator and report both the growth and evident debunching effects after saturation as measured for the first time. These results are discussed in relation to estimates of the bunching fraction calculated by GINGER [9] and used with an analytical model for nonlinear harmonic generation (NHG) [4].

Experimental Background

The experiments were performed at the Advanced Photon Source (APS) low-energy undulator test line (LEUTL) facility [10]. The S-band linear accelerator normally used for injection of beam into the storage ring was configured with the photocathode (PC) rf gun to provide the bright beams needed for SASE FEL operations. The electron beam energy was 217 MeV for FEL operations at the nominal 530-nm fundamental wavelength using the 3.3-cm period undulators with undulator parameter $K = 3.1$. The emittance was measured with a three-screen technique after the last accelerator, and beam energy and bunch length (using an rf zero-phasing technique [10]) were measured at a screen after a dipole at the end of the accelerator. The schematic of the gun, linac, diagnostics, and undulators is shown in Fig. 1. Table 1 summarizes the measured beam properties taken close in time to the gain scans.

Before and after each of the nine 2.4-m-long undulators, diagnostic stations are installed as described previously [11,12]. A combined quadrupole and corrector magnet is also located in each drift space. An actuator with YAG:Ce screen/mirror, 45° mirror only, and thin foil positions is located after the magnet and before the rf BPM. A CCD camera is used to view either SASE light reflected by the mirror or e-beam information from the YAG:Ce/mirror combination. Another moveable mirror at 45° to the beam direction is located 63 mm downstream from the first actuator. When this mirror is inserted by itself, the SASE radiation is directed to a second CCD camera, or visible light detector (VLD), mounted ~1.3 m away on the wall. Filter wheels are used to select bandpass filters or neutral density filters. When the upstream thin foil is inserted in combination with this 45° mirror, the COTR or OTR is imaged directly since the intense

SASE light is now blocked. The two surface sources, forward COTR from the thin foil and backward COTR from the pick-off mirror, combine to form the interference patterns at the mirror surface.

At the time of these experiments, four of the imaging stations (2, 4, 6, 8) for the second 45° pick off mirror had been upgraded to detect UV radiation down to 200 nm, the others remained as visible-light-only setups until the summer of 2001. The multiple filter wheels before the CCD camera were employed to position two solar blind (SB) bandpass filters that attenuate strongly any radiation longer than 360 nm and shorter than 225 nm. Neutral density filters were used to attenuate the 530-nm fundamental after all the stations, and then the SB filters were used to block the fundamental while allowing detection of the second harmonic at 265 nm. With the insertion of the 6- μm -thick Al foil just upstream, the same procedure was used for imaging the COTR. The imaging system was set up for near-field or far-field focus conditions by a translation stage that moved the CCD camera relative to the lens. In the near field the beam size at the 45° mirror surface is observed with the image from the surface 63 mm upstream being defocused. In the far-field focus, the angular distribution of the emitted radiation is observed. In the case of COTR it would include the interference from the two sources 63 mm apart. Experimentally, z-dependent intensity scans were taken on the SASE fundamental, COTR fundamental, SASE second harmonic, and COTR second harmonic. There were beam property measurements taken before and after the scans. Some drifts in the rf accelerator resulted in the bunch length variation during this time. The results of these measurements are discussed in the next section.

Experimental Results and Discussion

The data are from the March 30, 2001 run where high peak currents were used. Biedron et al. have previously reported the results of the SASE gain scans and GINGER calculations [6]. In this discussion we address the COTR and hence microbunching aspects. In Table 2 we list the results of the z-dependent intensity measurements for the COTR fundamental and second harmonic at stations VLD 2, 4, 6, and 8. The signal of the second harmonic was too weak for the automated program to process at VLD2 (a manual integration was done to generate an estimate), but we can take the ratio of the observed fundamental to second harmonic at three different z positions that are 4.8 m apart. There was a peak current change during the runs, so there is a caveat about the beam stability. In both wavelength cases though, the COTR signals are stronger at Station 6 and noticeably weaker at Station 8. We have maximal microbunching at Station 6, and then the debunching occurs as indicated by the COTR intensity reduction of a factor of 20-55. We note that the corresponding SASE gain scans at both wavelengths obtained on the same day do not exhibit such a dramatic decrease. Since the pick-off mirror reflects all the light out of the vacuum chamber and the same cameras are used, the COTR intensity effect must be real. The COTR1/COTR2 ratios are 71 and 100 for Stations 4, 6 and then it drops to 38 at Station 8. This indicates the fundamental component in the microbunching was reduced relatively faster than the second harmonic in our experimental conditions.

For completeness a similar tabulation for the SASE radiation is also presented in Table 2. In this case the SASE fundamental to second harmonic ratios are 175, 358, and 423 at Stations 4, 6, and 8, respectively. These data were compared to the results of

GINGER simulations for the nonlinear harmonic generation. Additionally, the analytical model of Huang and Kim [4] was used to estimate the radiation intensities based on the relationship of the fundamental energy E_1 and the second harmonic energy E_2 ,

$$E_2 \approx E_1 \left(\frac{K}{\gamma_0 k_u \sigma_x} \right)^2 \left(\frac{K_2}{K_1} \right)^2 \left(\frac{b_2}{b_1} \right)^2, \quad (1)$$

where K is the undulator parameter; γ_0 is the Lorentz factor of the electron beam; k_u is the wave number of the undulator period; σ_x is the average rms electron beam size in the wiggling plane; K_1 and K_2 are the effective coupling strength factors due to the fundamental and second harmonic radiation, respectively; and b_1 and b_2 are the microbunching factors of the electron beam at the fundamental and second harmonic wavelengths, respectively.

The bunching fractions for the COTR are estimated by using the GINGER output for the beam conditions given in Table 1. The qualitative agreement is shown in Fig. 2, where the square of the microbunching factors for the fundamental and second harmonic plus the COTR data are plotted versus z , the undulator length in meters. In both cases the postsaturation experimental intensities decrease faster than the simulation. Nonideal trajectories may cause such an effect. We also evaluated a method to estimate the SASE E_1/E_2 ratio by directly using the measured $\text{COTR}_1/\text{COTR}_2$ ratio. An additional reduction of $(1/n)^4$, where $n=2$ for the second harmonic intensity, is also predicted by equation 4 of Ref. 5 for COTR. The adjusted COTR harmonic ratio is used in our Eq. 1 instead of

$\left(\frac{b_2}{b_1} \right)^2$. After inserting the parameter values we can rewrite the relationship as

$$E_1/E_2 = A (\text{COTR}_1/\text{COTR}_2), \quad (2)$$

where $A = 6.5$ and 4.7 for the $\gamma\epsilon_x = 9$ and $\gamma\epsilon_x = 6.5$ cases, respectively. The resultant estimation is encouraging in the exponential regime since for Stations 4 and 6 we obtain measured E_1/E_2 ratios that are 2.5 and 3.5 times the COTR ratio, respectively. We note the GINGER simulations of the bunching factors were very similar for the two beam parameter conditions of Table 1.

Summary

In summary, we report the first z-dependent measurement of COTR harmonics, and we compare these to predictions of a simulation code and analytical model. Although the beam parameters did measurably change during the course of the experiments, this effect has been evaluated by use of the modeling to permit our cross-comparison of the measured SASE and COTR fundamental to second harmonic intensity ratios. Further experiments are needed and will be explored at 660 nm on the fundamental so that the third harmonic might also be detectable in the UV cameras.

Acknowledgements

The authors acknowledge the support of O. Singh, A. Raugas, R. Gerig, and E. Gluskin of the Advanced Photon Source.

Table 1: Electron beam parameters measured at the time of the gain scans for SASE and COTR.

Parameter	530-nm Gain Scan	265-nm Gain Scan
Beam Energy (MeV)	217	217
Peak Current (A)	505	360
Energy Spread (%)	0.1 – 0.2	0.1 – 0.2
Bunch Length (fs RMS)	150	200
Charge (pC)	190	180
Emittance x (mm mrad)	9.0	6.5
Emittance y (mm mrad)	8.0	7.1

Table 2: Results of COTR and UR measurements
for runs on March 30, 2001

Wavelength	Station	COTR Intensity ($\times 10^5$ counts)	Ratio 1 st /2 nd
530	VLD 2	7.8×10^{-2}	(33)
530	VLD 4	5.9	70
530	VLD 6	6.6×10^2	101
530	VLD 8	11.9	38
265	VLD 2	(2.4×10^{-3})	----
265	VLD 4	8.3×10^{-2}	----
265	VLD 6	6.6	----
265	VLD 8	0.32	----

Wavelength	Station	UR Intensity ($\times 10^5$ counts)	Ratio 1 st /2 nd
530	VLD 2	8.2	2.5
530	VLD 4	1,934	175
530	VLD 6	436,502	358
530	VLD 8	294,192	423
265	VLD 2	3.3	----
265	VLD 4	11.0	----
265	VLD 6	1,220	----
265	VLD 8	695	----

References

1. R. Bonafacio, L. Desalvo, P. Pierini, Nucl. Instrum. Methods A293, (1990) 627.
2. H.P. Freund, S.G. Biedron, S.V. Milton, IEEE J. Quantum Electron., 36 (2000) 275.
3. Z. Huang and K.-J. Kim, Phys. Rev. E 62, (2000) 7295.
4. Z. Huang and K.-J. Kim, Nucl. Instrum. Methods A475, (2001).
5. A. Tremaine et al., Phys. Rev. Lett. 88 (20), (2002) 204801.
6. S. Biedron et al., Nucl. Instrum. Methods A483, (2002) 94.
7. A. Tremaine et al., Phys. Rev. Lett. 81, (1998) 5816.
8. A. H. Lumpkin et al., Phys. Rev. Lett. 88 (23), (2002) 234801-1.
9. W. M. Fawley, A user manual for GINGER and its processor XPLOTGEN, LBNL-49625, 2002.
10. S.V. Milton et al., Nucl. Instrum. Methods A407, (1998) 210.
11. E. Gluskin et al., Nucl. Instrum. Methods A429, (1999) 358.
12. A.H. Lumpkin et al., Nucl. Instrum. and Methods A483, (2002) 402.

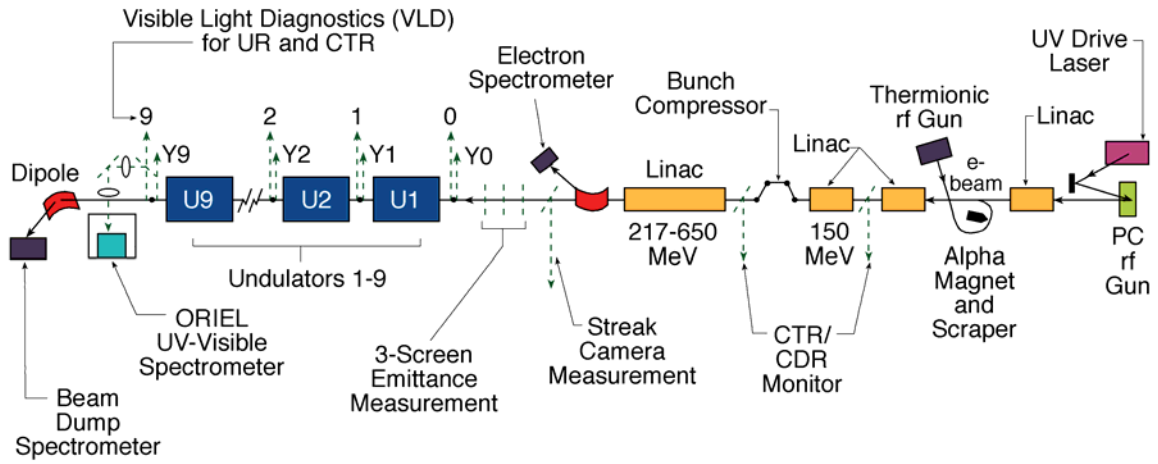
Figure Captions

Fig. 1 A schematic of the APS linac, diagnostics stations, and undulators in the LEUTL tunnel.

Fig. 2 A z-dependent comparison of the square of the microbunching factors calculated by GINGER and the corresponding COTR fundamental and second harmonic intensity data. Two SB filters were used in front of the camera to obtain the second harmonic

data cleanly.

Schematic of APS SASE FEL Experiment



AHL
9/28/00

Fig.1

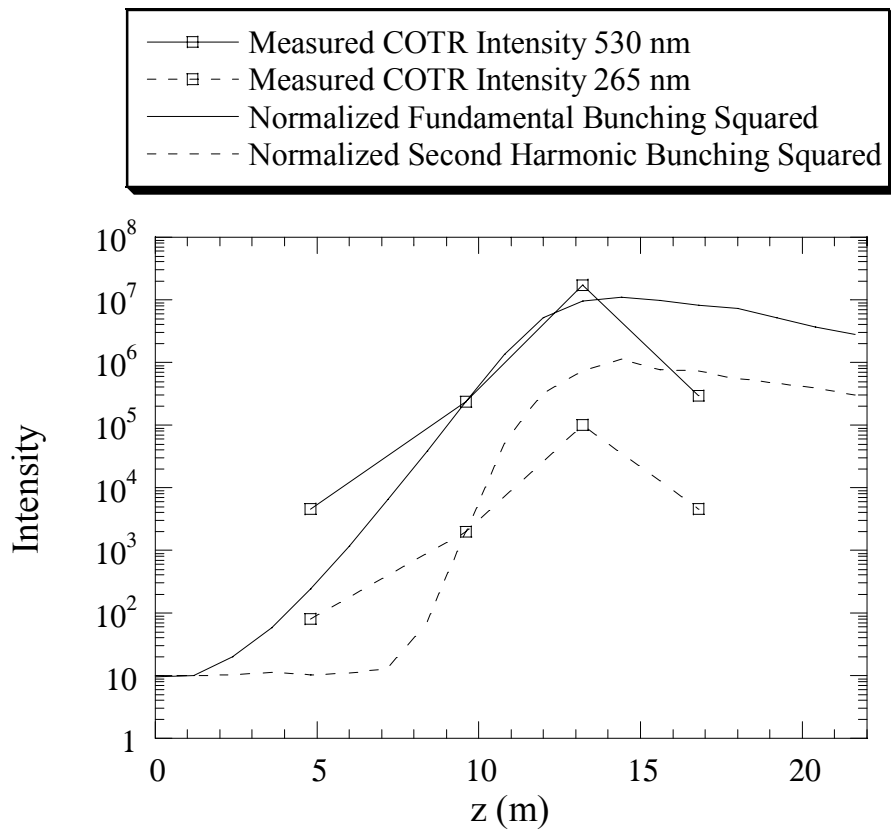


Fig.2